Heliyon 10 (2024) e35486

Contents lists available at ScienceDirect

Heliyon

journal homepage: www.cell.com/heliyon

Research article

Biogenic silver nanomaterials synthesized from *Ocimum sanctum* leaf extract exhibiting robust antimicrobial and anticancer activities: Exploring the therapeutic potential

Nayeem Ahmad [a], Mohammad Azam Ansari [b], Ali Al-Mahmeed [a], Ronni Mol Joji [a], Nermin Kamal Saeed [c], Mohammad Shahid [a,*]

[a] *Department of Microbiology, Immunology, and Infectious Diseases, College of Medicine & Medical Sciences, Arabian Gulf University, Bahrain*
[b] *Department of Epidemic Disease Research, Institute for Research and Medical Consultations (IRMC), Imam Abdulrahman Bin Faisal University, Dammam, Saudi Arabia*
[c] *Microbiology Section, Department of Pathology, Salmaniya Medical Complex, Bahrain*

ARTICLE INFO

Keywords:
Ocimum sanctum
OsAgNPs
Nanoparticles
Multidrug-resistant (MDR)
HeLa cancer cells

ABSTRACT

There is a surge in antibiotic consumption because of the emergence of resistance among microbial pathogens. In the escalating challenge of antibiotic resistance in microbial pathogens, silver nanoparticles (AgNPs)-mediated therapy has proven to be the most effective and alternative therapeutic strategy for bacterial infections and cancer treatment. This study aims to explore the potential of OsAgNPs derived from *Ocimum sanctum's* aqueous leaf extract as antimicrobial agents and anticancer drug delivery modalities. This study utilized a plant extract derived from *Ocimum sanctum* (Tulsi) leaves to synthesize silver nanoparticles (OsAgNPs), that were characterized by FTIR, TEM, SEM, and EDX. OsAgNPs were assessed for their antibacterial and anticancer potential. TEM analysis unveiled predominantly spherical or oval-shaped OsAgNPs, ranging in size from 4 to 98 nm. The (MICs) of OsAgNPs demonstrated a range from 0.350 to 19.53 μg/ml against clinical, multidrug-resistant (MDR), and standard bacterial isolates. Dual labelling with ethidium bromide and acridine orange demonstrated that OsAgNPs induced apoptosis in HeLa cells. The OsAgNPs-treated cells showed yellow-green fluorescence in early-stage apoptotic cells and orange fluorescence in late-stage cells. Furthermore, OsAgNPs exhibited a concentration-dependent decrease in HeLa cancer cell viability, with an IC50 value of 90 μg/ml noted. The study highlights the remarkable antibacterial efficacy of OsAgNPs against clinically significant bacterial isolates, including antibiotic-resistant strains. These results position the OsAgNPs as prospective therapeutic agents with the potential to address the growing challenges posed by antibiotic resistance and cervical cancer.

1. Introduction

Nanotechnology has become one of the most alluring fields of research, with its distinctive properties and wide-ranging uses in sectors as diverse as food, agriculture, and medicine [1]. Metal nanoparticles with multiple therapeutic applications include those

* Corresponding author. Department of Microbiology, Immunology, and Infectious Diseases, College of Medicine & Medical Sciences, Arabian Gulf University, Bahrain.
E-mail address: mohammeds@agu.edu.bh (M. Shahid).

https://doi.org/10.1016/j.heliyon.2024.e35486
Received 19 May 2024; Received in revised form 29 July 2024; Accepted 30 July 2024
Available online 31 July 2024

composed of silver, platinum, gold, copper, titanium, zinc, and magnesium. They have distinct physicochemical properties that make them ideal for a variety of biomedical uses, including antimicrobial, antioxidant, anticancer, antidiabetic, anticoagulant, and thrombolytic activities [2]. Both physical and chemical methods have been used to successfully synthesize nanoparticles. Although it is necessary to point out that this procedure does not connect with environmental sustainability, in this context, there has been a prominent significance to biological concepts for synthesizing metallic nanoparticles. These methods harness the power of biological resources, including microorganisms, marine algae, microfluidics, animal metabolites, and plant extracts, to effectively stabilize nanoparticles. The scientific community has given these biologically based techniques a lot of attention, and they provide an environmentally friendly alternative [3–5]. Although the microbial-based approach to producing nanoparticles indeed has limitations that include the requirement to preserve aseptic culture environments, low production quantities, and high costs, it is important to remember that plant-mediated nanoparticle synthesis is a very advantageous substitute. Furthermore, a wide range of biological activities is demonstrated by plant-mediated synthesis, which permits large-scale production [6–8]. When compared to traditional synthesis, green synthesis offers up to 40 % cost savings, a 30 % reduction in energy usage, and a 50 % boost in production [9].

Furthermore, plants are an excellent and easily obtainable source of bioactive secondary metabolites, such as proteins, terpenoids, polysaccharides, alkaloids, flavonoids, ketones, amines, and aldehydes. When metal ions are converted into metal nanoparticles, these substances act as reducing, capping, and stabilizing agents, producing the desired nanoparticles with predefined features [10]. The capacity of plant components to lower metal ions and promote the creation of nanoparticles has been explored, including leaves, roots, and seeds [9]. Furthermore, the phytochemicals from plant extracts can be inserted or attached to the outer surface of the nanoparticles in their development process, which is critical in their antimicrobial and anticancer-like biological applications [11]. Other biomedical applications of nanoparticles compromise antioxidants and drug delivery mechanisms [9].

Silver nanoparticles are among the many biosynthesized metal nanoparticles that were in high demand because of their unique and distinguishing qualities, such as high stability and conductivity [12]. AgNPs are produced by a two-step process that starts with the reduction of Ag + ions to Ag^0 and ends with agglomeration and stabilization, which produce colloidal AgNPs [13]. Even though silver is dangerous at higher concentrations, numerous studies have demonstrated that a lower concentration of $AgNO_3$ has superior chemical stability, biocompatibility, catalytic activity, and intrinsic therapeutic potential [14]. To produce environmentally beneficial nanoparticles, primary and secondary metabolites undergo continuous redox reactions. AgNPs have been synthesized from plants of *Boerhaavia diffusa* [15], *Silybum marianum* [16], *Urtica dioica* [17], *Elephan-topus scaber* [18], *Bergenia ciliate* [19], *Ocimum basilicum* [20], and *Azadirachta indica* [21].

Ocimum sanctum is also known as the "Queen of Herbs" due to its numerous health benefits, which include antiviral, antidiabetic, antistress, antioxidant, and antibacterial qualities. Among the most significant aromatic herbs, *Ocimum sanctum* is frequently utilized in the pharmaceutical sector. *It* is mostly utilized as an oil and extract. The primary secondary metabolites found in this extract include Eugenol, Linalool, β-Caryophyllene, Carvacrol, Apigenin, Rosmarinic Acid, and Urosolic Acid. These compounds are derived from *Ocimum sanctum* and other medicinal plants and include alkaloids, phenols, glycosides, flavonoids, tannins, saponins, terpenoids, steroids, and quinone [22,23]. Various analytical techniques, including nuclear magnetic resonance (NMR), gas or liquid chromatography-tandem to mass spectrometry, GC-FID, and many more, have been used in numerous investigations to identify them [24]. Numerous researches have documented the bioactivities and potential therapeutic benefits of the essential oils of African and Holy *Ocimum sanctum* [25].

In this study, the leaves of the *Ocimum sanctum* plant were selected for extracting active molecules, for green synthesis, and for use as an antimicrobial and anticancer agent. Harmful bacteria cause infections that affect millions of people worldwide, leading to a significant number of deaths. Overuse and misuse of antibiotics have resulted in drug resistance in various bacteria, making treatments ineffective against certain disease-causing germs. This has led to antibiotic resistance (AMR), which occurs when bacterial mutations reduce the effectiveness of antibiotics. AMR is currently one of the biggest threats to public health in the twenty-first century. According to the UK Government-commissioned Review on Antimicrobial Resistance, AMR may cause up to 10 million annual deaths by 2050 [22,26]. Throughout human history, medicinal herbs have been utilized to address a variety of health conditions. As a result, plant-based silver nanoparticles have become a promising solution for combating pathogenic bacteria that have grown resistant to traditional antibiotics. The efficacy of these nanoparticles can be attributed to the presence of essential metabolites within the plant extract. A study in India by Ramamurthy et al. reported that at 1 % and 2 %, *Ocimum sanctum* demonstrated significant antibacterial action against Black Pigmented Bacteroides [27]. Another study also reported that *Ocimum sanctum* extract inhibited the growth of Gram-positive and Gram-negative bacterial strains [28].

Cancer is a devastating and widespread illness that claims countless lives across the globe. The disease arises when cells or tissue grow abnormally and divide uncontrollably, increasing the number of cell divisions [29]. Although there are various treatment options available, including immunotherapy, chemotherapy, surgery, and radiotherapy, cancer continues to pose a significant challenge due to its high mortality rate and rapid spread [30]. Cancer cells can evade apoptosis, the natural process of cell death, resulting in uncontrolled multiplication. The primary objective of cancer therapy is to address this characteristic of cancer cells. Plant-based nanosized silver has emerged as a popular approach to battle cancer. Studies have revealed that the mechanism behind this involves the induction of apoptosis through mitochondrial depolarization and DNA damage. An elevation in ROS, cell cycle arrest, and caspase-3 activation collectively contribute to the elimination of cancer cells [31]. Developing effective medications that can accurately target specific areas is vital. Nanoparticle therapy is a promising option for treating cancer. Silver nanoparticles synthesized from plant extracts have demonstrated potential in combating various types of carcinoma cells [32]. By interrupting the cell cycle, environmentally friendly silver nanoparticles can hinder cancer cell growth and possess anticancer properties [33]. According to recent research, AgNPs have been found to negatively affect mitochondrial function, resulting in a rise in ROS levels within cells. This elevation in oxidative stress is believed to be the main reason why cells are damaged. Furthermore, AgNP's large surface area makes it

easy to enter cells and interact with several cellular structures, which stops the cellular signalling cascade. Excitingly, plant-based AgNPs have the potential to develop into novel antibiotics against bacterial infections. They can also result in significant advancements in cancer treatment by reducing DNA damage and reactive oxygen species formation. *Ocimum sanctum* leaves were found to drastically lower the occurrences of hematoma and squamous cell carcinoma in experimental rats, according to research by Aruna et al. [34].

According to Luke et al. study, *Ocimum sanctum* is cytotoxic to the Ca9-22 cell line, which is used to examine oral squamous carcinoma. This plant's leaves contain phytochemicals that give it the ability to combat oral cancer [35]. Most of the existing studies on *Ocimum sanctum* have focused on the plant and its extracts from other parts of the world, including India, where it is widely used as a medicinal herb [36,37]. This study utilized *Ocimum sanctum* leaves collected from the local region, which is a novel contribution. Exploring *Ocimum sanctum* sourced from the local area provides new insights and perspectives, as the therapeutic potential can be influenced by the specific growing conditions and environment.

Our research focuses on the synthesis and characterization of silver nanoparticles derived from the *Ocimum sanctum* plant (OsAgNPs) using TEM, SEM, FTIR, and EDX techniques. To verify our results, we conducted tests on a variety of bacterial strains, including clinical, standard, and multidrug-resistant isolates, where the specific antibiotic resistance mechanisms were identified [38,39] through molecular methods, to assess the antibacterial properties of the OsAgNPs which is a novel contribution. Additionally, we evaluated the effect of freshly produced OsAgNPs on HeLa cells, utilizing cell morphology and MTT assays to determine cell survival rates. We also investigated the potential of AgNPs to induce apoptosis through cell cycle analysis and dual AO/EtBr labelling. Our objective is to explore the potential of OsAgNPs derived from *Ocimum sanctum's* aqueous leaf extract as both antimicrobial agents and anticancer drug delivery modalities by examining their antibacterial and anticancer properties.

2. Material methods

2.1. Laboratory reagents, plant material and bacterial strains

High-quality $AgNO_3$ was procured from Surechem (SCP) Products LTD, England, and all analytical reagents, as well as microbial media, were obtained from Hi-Media. The synthesis of silver nanoparticles involved the collection of *Ocimum sanctum* leaves from a young plant situated at the Arabian Gulf University campus in Manama, Kingdom of Bahrain. Bacterial strains were sourced from the repository of the Department of Microbiology, Immunology & Infectious Diseases at the College of Medicine & Medical Sciences, Arabian Gulf University. Clinical strains, encompassing both susceptible and multi-drug-resistant variants, were acquired from the Section of Microbiology at Salmaniya Medical Complex. This comprehensive sourcing strategy ensured the use of well-characterized materials and microbial strains in the experimental procedures.

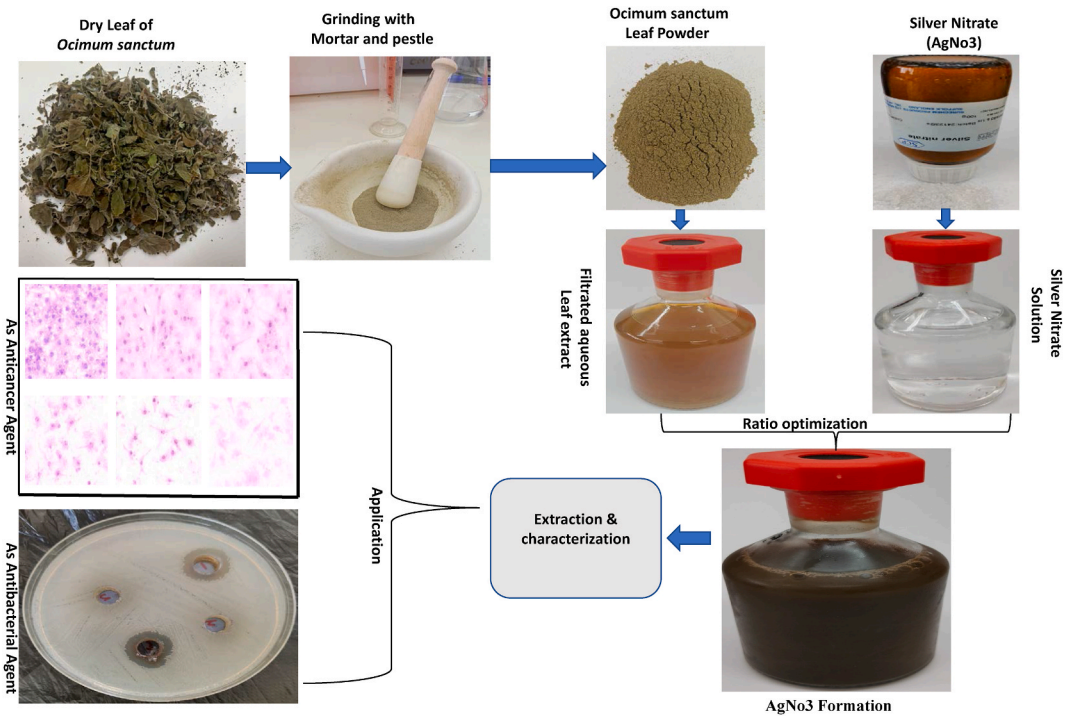

Fig. 1. Schematic representation of green synthesis of silver nanoparticles.

2.2. Aqueous extract preparation of the Ocimum sanctum leaf

Before being utilized in research, the *Ocimum sanctum* leaves underwent a meticulous cleaning process using distilled water to remove any surface impurities or dirt. Following this, the leaves were sundried until completely devoid of moisture. The subsequent step involved grinding the thoroughly dried leaves into an exceptionally fine powder using a mortar and pestle. To generate the aqueous extract, 10 g of the dried powder was blended and transferred to 100 ml of deionized water in a 250 ml reagent bottle. The extract was then passed using Whatman No. 1 filter paper (sourced from Maidstone, UK) and a 0.22 μm filter (supplied by Millipore). Furthermore, the resulting aqueous extract was stored at 4 °C for further experiments.

2.3. Synthesis of silver nanoparticles

In the experiment, a 1 mM silver nitrate solution was combined with an aqueous leaf extract in a ratio of 95 ml–5 ml. Within 24 h, the solution's colour changed from colourless to brown, indicating that Ag^+ had reduced to Ag^o as shown in (Fig. 1). The next step involved collecting the green AgNPs by centrifuging the solution at 13,000 rpm for 60 min. The pellets were rinsed three times with deionized water to eliminate any excess silver ions. Lastly, the AgNPs were lyophilized and kept for later use and characterization at room temperature in screw-capped vials.

2.4. Characterization of synthesized nanoparticles

2.4.1. Fourier-transform infrared (FTIR)

The capping and effective stability of synthesized silver nanoparticles (OsAgNPs) were investigated using Fourier-transform infrared (FTIR) spectroscopy to identify potential functional groups within *Ocimum sanctum* leaf extract (Cary 630 Agilent, Stevens Creek Blvd., Santa Clara, CA, USA). An FTIR spectrum obtained in the diffuse reflectance mode with a resolution of 4 cm^{-1} covered the 400–4000 cm^{-1} range [40].

2.4.2. Analysis by scanning electron microscopy (SEM) and energy dispersive X-ray (EDX)

A uniform layer containing OsAgNPs was placed onto glass coverslips, forming films, for analyzing the surface morphology of the nanoparticles. The sample was then treated with a gold-coating sputter. This procedure made use of a JEOL electron microscope (JSM6390LV, Japan) in conjunction with the WINDOW BAS software. Furthermore, energy-dispersive X-ray spectroscopy (EDX) was used to discern and recognize the elemental constituents present in the OsAgNPs, contributing to a thorough understanding of their chemical composition [40].

2.4.3. Transmission electron microscopy (TEM)

The shape and size of the green-synthesized OsAgNPs were determined using transmission electron microscopy (TEM) on a Jeol 2100 instrument from Tokyo, Japan. A small amount of the synthesized OsAgNPs was placed onto a copper grid (Sigma-Aldrich, St. Louis, MO, USA) and allowed to dry. After drying, the samples were placed in a transmission electron microscope, which used electronic radiation to illuminate the sample under vacuum conditions [41].

2.5. Antibacterial potential of biogenically synthesized nanomaterials

2.5.1. Zone of inhibition assay

The antibacterial potential of biogenically produced nanomaterials was assessed against clinical, multidrug-resistant (MDR), and standard bacterial isolates. The specific antibiotic resistance mechanisms in the clinical and MDR isolates were identified through molecular methods [38,39]. These clinical and MDR isolates included in this study were carbapenem-resistant, colistin-resistant, or cephalosporin-resistant bacteria, which are particularly challenging-to-treat organisms Growth inhibition experiments were conducted using the Kirby-Bauer diffusion method on a solid agar medium. The isolates were cultured for 18 h, and an inoculum suspension of 0.5 McFarland Units was prepared. Subsequently, a bacterial suspension was spread onto Mueller Hinton Agar (MHA) media and swabbed across the entire plate. The bacterial suspension was absorbed by every plate, and at different locations, 8 mm-diameter wells were punched into the agar media. OsAgNPs suspensions in 100 μl volumes were added to each well in the plate, along with leaf extract used as a negative control. The plates were then incubated at 37 °C overnight. DDW was used as a negative control.

2.5.2. Minimal inhibitory concentrations (MICs) and minimum bactericidal concentration (MBC)

The broth micro-dilution method was used by CLSI guidelines to determine the minimal inhibitory concentrations (MICs) for the tested OsAgNPs against clinical, multidrug-resistant (MDR), and standard bacterial strains. 100 μL of Muller-Hinton broth were dispensed into 96 multi-well microtiter ELISA plates. OsAgNPs serial dilutions were performed twice. A previously prepared bacterial suspension was adjusted for optical density at 600 nm to produce a turbidity of 0.5 McFarland standard, equivalent to 10^8 CFU/ml, to prepare a bacterial inoculum. This suspension was diluted further and inoculated at a final concentration of 5×10^5 CFU/ml in all plates. Each plate contained both positive and negative controls. Furthermore, the microtiter plates were incubated at 37 °C for 24 h before being visually inspected for the presence or absence of turbidity against a dark background. When compared to the control, the MIC was determined as the lowest concentration of OsAgNPs that showed no visible bacterial growth. Furthermore, 20 μL from each of

the wells with no visible bacterial growth were inoculated on the surface of agar plates and incubated overnight at 37 °C to determine the minimum bactericidal concentration (MBC), defined as the lowest concentration of OsAgNPs that kills more than 99.9 % of the initial bacterial inoculum.

2.6. Cell line source and culture

We purchased the HeLa cell line (Cat. # CCL-2™) from the American type culture collection (ATCC) https://www.atcc.org/products/ccl-2. The cells were cultured as manufacturer protocols at 37 °C in a humidified environment with 5 % carbon dioxide in Dulbecco's Modified Eagle Medium (DMEM) supplemented with 10 % fetal bovine serum (FBS). The cells were trypsinized using a buffered saline solution that contained 0.25 % (w/v) trypsin and 0.03 % EDTA once they reached 70 % confluence. The cells were then plated onto the culture plate in the desired pattern and allowed to adhere for 24 h.

2.6.1. Cytomorphological changes in HeLa cancer cells by OsAgNPs

HeLa cells (1×10^5 cells/well) were placed in a six-well plate and incubated for 24 h. After 24 h, cells were treated with 15, 30, 60, 90, and 120 g/mL of synthesized OsAgNPs and incubated at 37 °C in a 5 % CO_2 atmosphere for another 24 h. Following the time of incubation, the cells were washed twice with PBS, and a phase contrast microscope (CTR 6000; Leica, Wetzlar, Germany) was used to view and capture any morphological changes in the cells.

2.6.2. The cell viability assay

The viability of the treated and untreated cells was examined using an MTT assay. Thiazolyl Blue Tetrazolium Bromide (MTT) is a yellow dye that is converted into formazan by the enzyme mitochondrial dehydrogenase. In the assay procedure, 96-well plates were seeded with 10^4 cells per well and then let for adhesion overnight. The medium was then taken out and the cells were incubated for 24 h at 37 °C with different concentrations of OsAgNPs. Subsequently, the cells were subjected to MTT dye (5 mg/ml in PBS) for 4 h after the treatment. Following a 10-min incubation period, 200 µl of dimethyl sulfoxide (DMSO) was added to dissolve the formazan crystals. A Genetix580 microplate reader (USA) was then used to measure the absorbance at 490 nm. Simultaneously conducted under identical conditions, untreated sets were used as controls. Finally, the following formula was used to convert the cultures' optical density (OD) values into a percentage of viability.

$$\textit{Cell viability}\ (\%) = \left[\frac{OD_{sample}}{OD_{Control}}\right] \times 100$$

2.6.3. Apoptosis assay by acridine orange/ethidium bromide staining

HeLa cells were subjected to different time intervals of 15 and 30 µg/ml of OsAgNPs. 1 µl of acridine orange/ethidium bromide

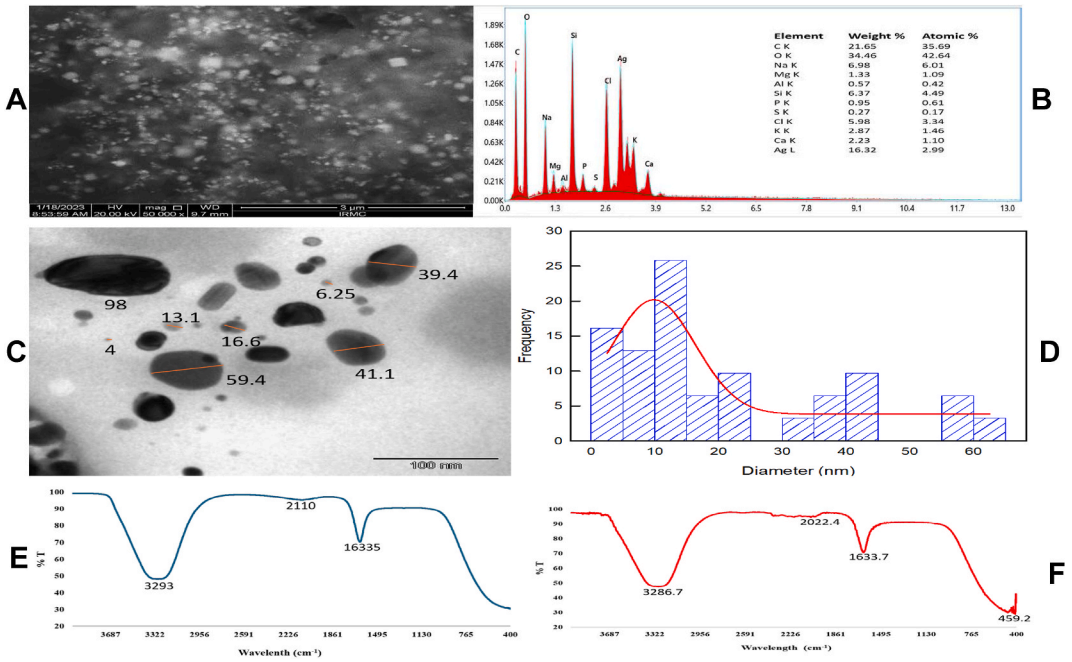

Fig. 2. Characterization of synthesized *Ocimum sanctum* silver nanoparticles: (A) SEM image at higher magnification, (B) EDX spectra, (C) TEM image, (D) particle size distribution, (E) FTIR analysis of *Ocimum sanctum* leaf extract and (F) FTIR analysis of synthesized OsAgNPs.

solution (one part each of 100 μg/ml acridine orange and 100 μg/ml ethidium bromide in PBS) was incubated with a 100 μl aliquot of the treated cells (approximately 1×10^5 cells/ml) before microscopy assessment. A 10 μl aliquot of the carefully blended mixture was put on microscope slides and covered with glass slips before being examined under a fluorescence microscope. Ethidium bromide selectively stained cells that had lost membrane integrity, but acridine orange stained both living and dead cells. Live cells exhibited a uniform green fluorescence, distinguishing them from apoptotic cells, which displayed a yellow to orange colouration indicative of varying degrees of membrane integrity loss due to co-staining with ethidium bromide. This dual-staining approach allowed for the visualization, differentiation of live, and apoptotic cells.

3. Results

3.1. Bio-reduction and synthesis of Ag NPs

Ocimum sanctum leaf extracts were used to synthesize Ag NPs; a formation of a brownish colour was observed immediately after adding phytoextracts to 1 mM silver nitrate ($AgNO_3$) due to the bio-reduction of silver (Ag+) ions into silver nanoparticles (Ag NPs). 1 mM $AgNO_3$ with phytoextracts produced a dark-brown colour, confirming the formation of Ag NPs because of Ag + reduction, color development was accelerated gradually. The colour of the reaction mixture changed from yellow-brown to darkish-brown during the synthesis of OsAgNPs due to the presence of biomass, which plays an important role in the biosynthesis of OsAgNPs (Fig. 1).

3.2. Scanning electron microscopy (SEM) and energy dispersive X-ray (EDX)

The investigation into the morphological, dimensional, and elemental attributes of powdered OsAgNPs was conducted through the integration of SEM in conjunction with EDX. High-resolution images were accurately captured (magnifications ×50000), affording a granular portrayal of the nanoparticles (Fig. 2A). The validation of silver signals was accomplished by subjecting the sample to EDS spectrometric analysis. Notably, the silver signal exhibited a discernible peak at three keV, conclusively affirming the elemental presence of silver. Moreover, the identification of additional elements, specifically oxygen and carbon, was attributed to the manifestation of confined surface plasmons. The quantitative composition, expressed in weight per cent, revealed carbon, oxygen, and silver at 21.65 %, 34.46 %, and 16.32 %, respectively as delineated in (Fig. 2B).

3.2.1. Transmission electron microscopy (TEM)

The morphology and size of OsAgNPs were determined using a transmission electron microscope. The dispersed particles had a spherical shape, indicating a large surface area within the produced nanostructures. The nanoparticles that formed ranged in size from 4 to 98 nm (Fig. 2C). The particle size distribution curve analyzed by ImageJ shows an average particle size of 10 nm. The TEM images of OsAgNPs indicated primarily spherical and oval forms (Fig. 2D).

3.2.2. FTIR analysis

FTIR spectrum of synthesized OsAgNPs is displayed in (Fig. 2E) and *Ocimum sanctum* leaf extract is displayed in (Fig. 2F). The spectrum reveals various vibration modes that confirm the existence of distinct functional groups within the OsAgNPs. Specifically, IR peaks at 3286.7, 2022.4, 1633.7, and 459.2 $cm^{-}1$ were identified in the OsAgNPs.

3.3. Antibacterial potential of nanoparticle

3.3.1. Zone of inhibition assay

The zone of inhibition (mm) against silver nanoparticles provides important insights into the nanoparticles' antimicrobial efficacy against multiple strains of bacteria. *Shigella sonnei* (ATCC 9290) showed a significant inhibition zone of 18 mm, indicating a significant impact on bacterial growth. *Enterococcus faecalis* (ATCC 29212) showed an even larger inhibition zone of 22 mm, demonstrating the silver nanoparticles' potent antimicrobial effect against this strain of bacteria. The zones of inhibition for *Staphylococcus aureus* (ATCC 25923) and methicillin-resistant *Staphylococcus aureus* (MRSA) were 24 mm and 12 mm, respectively. This indicates that although the standard *S. aureus* strain was effectively inhibited by the nanoparticles, the MRSA strain showed a slightly decreased susceptibility. The potential for efficiency of silver nanoparticles against *Pseudomonas aeruginosa* (ATCC 27853) and its carbapenem-resistant counterpart (CR) was highlighted by their corresponding inhibition zones of 20 mm and 16 mm. A consistent antimicrobial activity was observed against various *Escherichia coli* strains, as evidenced by the inhibition zones of 17 mm–21 mm observed in the NCTC-12900, clinical, carbapenem-sensitive (CS), and carbapenem-resistant (CR) bacterial strains. The susceptibility of the *Klebsiella pneumoniae* strains varied, with inhibition zones measuring between 12 and 17 mm. With a slightly smaller inhibition zone of 14 mm, the carbapenem and colistin-resistant (CRCsR) appeared to have a mild impact on its growth. *A. baumannii* strains (ATCC-19606, CS, CR) consistently demonstrated inhibition zones ranging from 17 mm to 22 mm, highlighting the broad-spectrum effectiveness of silver nanoparticles against this genus. However, *Serratia marcescens* (CR) displayed a comparatively smaller inhibition zone of 11 mm, indicating a potential limitation in the antimicrobial efficacy of silver nanoparticles against this particular strain. These findings understand the differential susceptibility of bacterial strains to silver nanoparticles, emphasizing their potential as effective antimicrobial agents against a range of clinically relevant pathogens (Table 1).

3.3.2. The Minimum Inhibitory Concentrations (MICs) and minimum bactericidal concentrations (MBCs)

To further evaluate biogenic nanomaterials against a battery of clinically significant multidrug-resistant and standard bacterial strains, the minimum inhibitory concentration (MIC) and minimum bactericidal concentration (MBC) were determined. *Enterococcus faecalis* (ATCC 29212) showed values of 0.61 for both MIC and MBC, whereas *Shigella sonnei* (ATCC 9290) showed values of 2.44 and 4.88, respectively. The *Staphylococcus aureus* (ATCC 25923) had found the MIC and MBC values of 0.305. MIC and MBC values for the methicillin-resistant *Staphylococcus aureus* (MRSA) strain were notably elevated at 19.53. Both the MIC and the MBC values for *Pseudomonas aeruginosa* (ATCC 27853) were 1.22 and 2.44, respectively, whereas the carbapenem-resistant (CR) strain had increased values of 4.88 and 9.765. The findings highlight the varying susceptibility of different bacterial strains to the tested biogenic nanomaterial, shedding light on its potential antimicrobial efficacy across a wide range of bacterial strains (Fig. 3).

3.4. Cytomorphological changes of HeLa cells induced by OsAgNPs

Morphological assessments of HeLa cancer cells were conducted and captured through a phase-contrast microscope. Morphological changes were evident in both control and HeLa cancer cells treated with OsAgNPs. The HeLa cells underwent treatment with OsAgNPs at concentrations of 15, 30, 60, 90, and 120 μg/mL for 24 h, revealing notable alterations characteristic of apoptotic cells. These changes included the loss of membrane integrity, cellular shrinkage, and a reduction in cell density, as depicted in the accompanying (Fig. 4).

3.4.1. Cytotoxicity assays

The *in-vitro* cytotoxic activity of silver nanoparticles against HeLa cell lines was assessed, revealing concentration-dependent cytotoxic effects. The MTT assay results demonstrated a decrease in cell viability over time with increasing concentrations of OsAgNPs, highlighting a time-dependent cytotoxicity. The reduction in MTT absorbance was inversely proportional to the escalating concentrations of OsAgNPs, indicating a dose-dependent impact on HeLa cancer cells. The half-maximal inhibitory concentration (IC50) of the biosynthesized OsAgNPs against HeLa cells was determined to be 90 µg/mL, as depicted in (Fig. 5), providing quantitative insight into the potency of the nanoparticles in inhibiting the growth of cervical cancer cells.

3.4.2. Dual AO/EtBr staining to detect apoptosis

Using dual acridine orange/ethidium bromide (AO/EtBr) staining, the apoptotic capability of OsAgNPs was demonstrated. Green fluorescence was observed exclusively in the untreated cells. Nevertheless, early-stage apoptotic cells showed crescent-shaped or granular yellow-green acridine orange nuclear staining upon treatment with OsAgNPs. Focused and irregularly localized orange nuclear ethidium bromide staining determined late-stage apoptotic cells. The apoptotic potential of OsAgNPs was substantiated through dual acridine orange/ethidium bromide (AO/EtBr) staining. In contrast, necrotic cells displayed an increase in volume and

Table 1
Size of the zone of inhibition against OsAgNPs.

Bacterial Strain	Zone of Inhibition (mm)
Shigella sonnei (ATCC 9290)	18
Enterococcus faecalis (ATCC 29212)	22
Staphylococcus aureus (ATCC 25923)	24
Staphylococcus aureus (MRSA)	12
Pseudomonas aeruginosa (ATCC 27853)	20
Pseudomonas aeruginosa (CR)	16
Escherichia coli (NCTC 12900)	21
Escherichia coli (clinical)	17
Escherichia coli (CS)	17
Escherichia coli (CR)	18
Klebsiella pneumoniae (ATCC 700603)	17
Klebsiella pneumoniae (Clinical)	17
Klebsiella pneumoniae (CRCsR)	14
Klebsiella pneumoniae (CRCsR)	14
Klebsiella pneumoniae (CRCsS)	15
Klebsiella pneumoniae (CRCsS)	12
Acinetobacter baumannii (ATCC 19606)	21
Acinetobacter baumannii (CS)	22
Acinetobacter baumannii (CS)	20
Acinetobacter baumannii (CR)	17
Acinetobacter baumannii (CR)	21
Serratia marcescens (CR)	11
DDW	8[a]

Abbreviations: (CS); carbapenem-sensitive (CR); carbapenem-resistant, (CRCsR); carbapenem and colistin-resistant, CRCsS; carbapenem-resistant and colistin-sensitive.
DDW: Double distilled water.
[a] 8 mm was the size of the punch well in agar. There was no obvious zone of inhibition beyond the well.

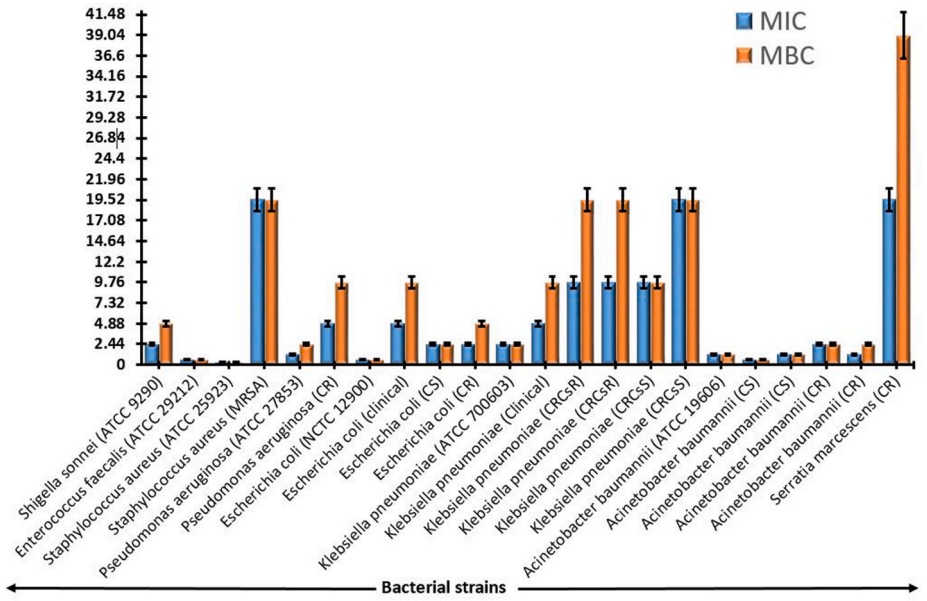

Fig. 3. The MICs and MBCs of OsAgNPs against clinical, multidrug-resistant, and standard bacterial strains.

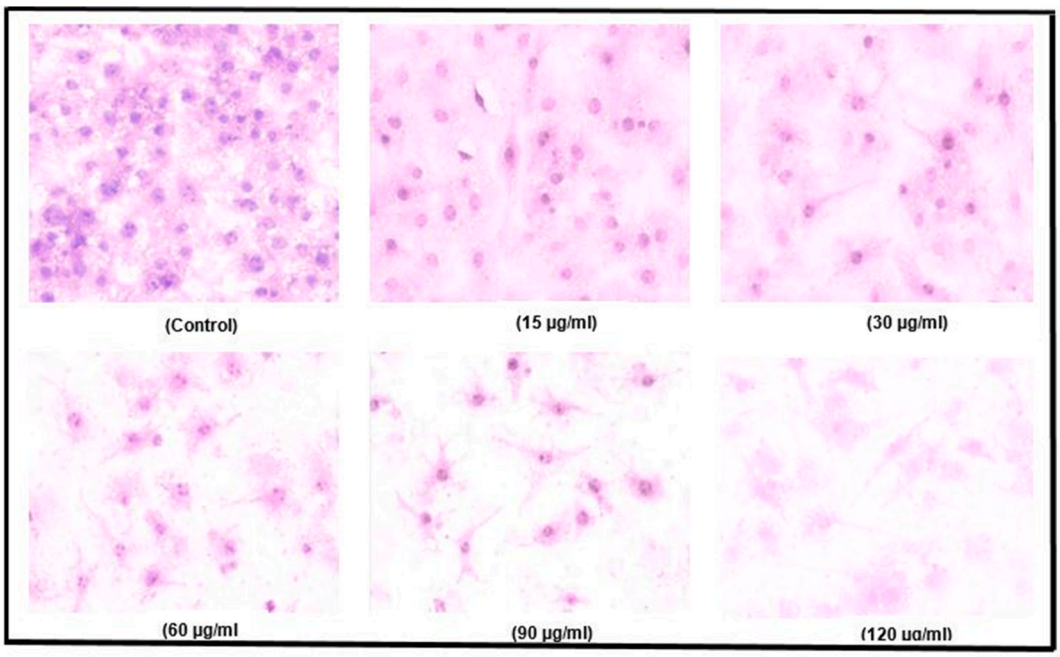

Fig. 4. Morphological examination of HeLa cancer cell after treatment with varying concentrations of OsAgNPs for 24 h.

manifested irregular, orange-red fluorescence at their periphery, as illustrated in (Fig. 6). This staining pattern provides visual evidence of the apoptotic and necrotic effects induced by OsAgNPs on the cellular structure.

4. Discussion

4.1. Plant extract synthesis of nanoparticle and its characterization

A rapid synthetic procedure for newly synthesized *Ocimum sanctum* silver nanoparticles OsAgNPs has been produced. Despite the absence of in-depth mechanism studies, the field of green synthesis often lacks comprehensive investigations into cytotoxicity.

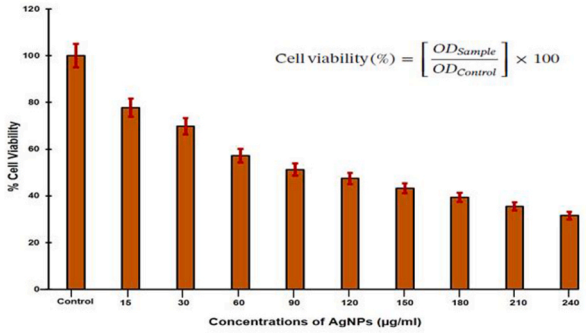

Fig. 5. Cell viability (MTT assay) of HeLa cancer cell lines *in vitro* when exposed to OsAgNPs.

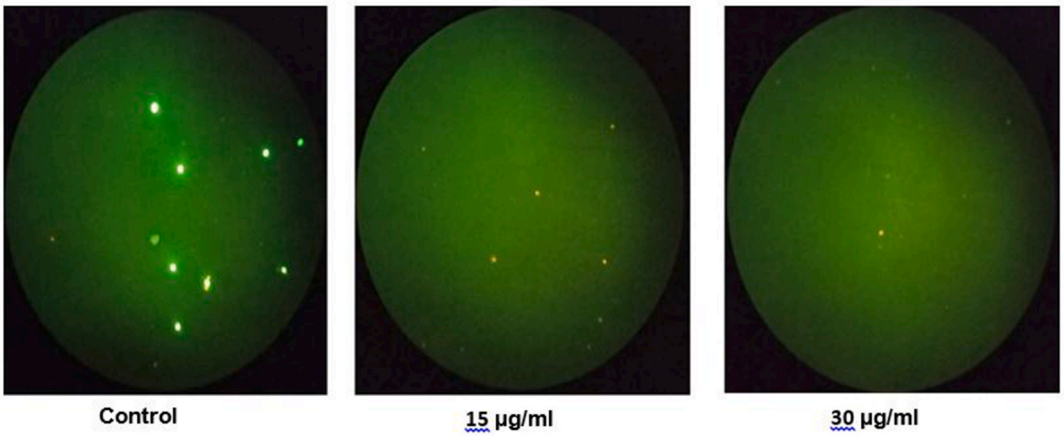

Fig. 6. The control demonstrated only green fluorescence while OsAgNPs treated in early-stage apoptotic cells became yellow-green (15 µg/ml) and late-stage became orange (30 µg/ml) due to necrosis, this was concentration dependent.

Originally, the method aimed to yield OsAgNPs with enhanced biocompatibility compared to chemically synthesized counterparts, thus avoiding cytotoxicity assessments. The development of OsAgNPs was promptly evidenced by a noticeable shift in solution colour, transitioning from yellow-brown to dark brown. This phenomenon is attributed to the rapid reduction of silver ions and the subsequent stabilization of OsAgNPs through biomolecules.

Analysis using Fourier-transform infrared (FTIR) spectroscopy revealed strong absorption peaks at 3286.7, indicative of the hydroxyl group associated with the polyphenolic component in the *Ocimum sanctum* leaf extract. Previous research has documented the abundance of polyphenols and flavonoids in *Ocimum sanctum* leaf extracts [42]. The peak observed at 1633.7 cm−1 is attributed to the presence of carbonyl groups (C=O) in polyphenolic compounds like luteolin, apigenin-7-O–D-rutinopyranoside, galuteolin, 4-hydroxybenzaldehyde, caffeic acid, gallic acid, chlorogenic acid, apigenin, and sumaresinolic acid within the leaf extract [42,43].

Table 2
Characteristics of biogenically synthesized OsAgNPs.

Biogenic OsAgNPs	Features
Source	*Ocimum sanctum*
Synthesis method	Bottom-up approach
Stabilizing/capping agent	Aqueous leaves extract
Preparation period	24 h
Nanoparticle size	4–98 nm
Stability	90 days
Phase	dark-brown colloidal
Biocompatible	Positive
Anticancer (IC_{50})	90 µg/ml against HeLa cells (ATCC CCL-2)
Antibacterial	*Shigella sonnei* (ATCC 9290), *Enterococcus faecalis* (ATCC 29212), *Staphylococcus aureus* (ATCC 25923), *Staphylococcus aureus* (MRSA), *Escherichia coli* (NCTC 12900), *Escherichia coli* (MDR), *Klebsiella pneumoniae* (ATCC 700603), *Klebsiella pneumoniae* (MDR) *Pseudomonas aeruginosa* (ATCC 27853), *Pseudomonas aeruginosa (MDR), Acinetobacter baumannii* (ATCC 19606) and *Acinetobacter baumannii* (MDR).

Furthermore, the peak at 2022.4.cm-1 is associated with CC stretching [44,45]. The peak at 459.2 cm−1 is related to the bonding of oxygen from the OH groups. These distinctive peaks of absorption indicated that the surface of AgNPs entailed phytochemicals derived from leaf extracts (polyphenols, flavonoids, alkaloids, amino acids, carbohydrates, etc.) that effectively stabilised and capped AgNPs, preventing them from aggregating [46]. Scanning electron microscopy (SEM) and transmission electron microscopy (TEM) were used to examine the surface morphology of the biogenic nanomaterials (Fig. 2A and C). The vacuum oven-dried materials were affixed to the SEM grid and examined at a magnification of ×50000. The analysis of the elements was performed using coupled energy-dispersive X-ray diffraction (EDX), which revealed the highest percentages of carbon, oxygen, and silver, respectively, of 21.65 %, 34.46 %, and 16.32 % (Fig. 2B). The elevated levels of carbon and oxygen suggest the biological origin of the synthesized material. Furthermore, the biogenic NPs were examined using TEM, which revealed spherical and oval form morphology with an average particle size of ~ 10 nm as analyzed by ImageJ (Fig. 2D and Table 2). The identified size of the synthesized AgNPs is consistent with the findings of Daniel et al. [47] where the size of AgNPs synthesized by *Ocimum tenuiflorum* was 20 nm and Alsalhi et al. [48], who also reported 20–30 nm AgNPs derived from rose petal extract [48]. Thus, the physical properties such as the size and shape of NPs and other functional properties of the produced AgNPs are significantly influenced by the nature of biomolecules utilized for capping and reduction [46].

4.2. Antimicrobial potential of silver nanoparticles (OsAgNPs)

The biogenic silver nanoparticles (AgNPs) response to various bacterial strains was measured, and the resulting MIC and MBC values offer important new information about the possible antimicrobial efficacy of the particles. *E. faecalis* (ATCC 29212) and *S. aureus* (ATCC 25923) show lower MIC and MBC values, indicating a relatively higher sensitivity to the silver nanoparticles. The findings show a spectrum of susceptibility among the tested strains. On the other hand, the literature's findings regarding the elevated MIC and MBC values for methicillin-resistant *S. aureus* (MRSA) underscore the ongoing challenge of antimicrobial resistance [49]. The differences in responses observed in carbapenem-resistant (CR) *P. aeruginosa* and carbapenem and colistin-resistant (CRCsR) *K. pneumoniae* highlight the biogenic nanomaterial's potential against multidrug-resistant (MDR) bacterial strains. These findings are consistent with recent studies that highlight the promise of nanomaterials in combating antimicrobial resistance [50]. Furthermore, the increased MIC and MBC values for carbapenem-resistant (CR) *S. marcescens* indicate a lower susceptibility, necessitating further research into alternative strategies for combating this resilient pathogen.

The reported Minimum Inhibitory Concentrations (MICs) of silver nanoparticles against a diverse range of bacterial strains in the study significantly contribute to our understanding of the antimicrobial potential of OsAgNPs. The concentration-dependent inhibition of bacterial growth, spanning from 0.305 to 19.53 μg/mL, underscores the versatility of OsAgNPs as potent antimicrobial agents as shown in (Fig. 3). As demonstrated by Dakal et al. [51], the exceptionally low MIC of 0.305 μg/mL against *S. aureus* (ATCC 25923) is consistent with earlier research highlighting the effectiveness of AgNPs against Gram-positive bacteria. The potential of AgNPs in combating a wide range of bacterial pathogens is further highlighted by the varied MIC values against *E. coli, K. pneumoniae, S. sonnei, E. faecalis,* MRSA, *A. baumannii*, and *P. aeruginosa* [52,53].

The results demonstrate that OsAgNPs have antimicrobial potential and can effectively combat clinically relevant strains as well as isolates that are resistant to multiple drugs. This improves the increasing corpus of research highlighting AgNPs' antimicrobial capabilities as a viable substitute for traditional antibiotics [54]. The significance of having a sophisticated understanding of OsAgNPs' interactions with various microbial entities is highlighted by the different MIC values amongst bacterial strains. Future research could examine potential synergies with current antibiotics and delve into the mechanistic aspects of OsAgNPs' antimicrobial action. Translational research would also greatly benefit from studies on the safety profile of OsAgNPs and their possible clinical uses, such as in wound care or medical device coatings. The findings are consistent with previous research on the antimicrobial properties of silver nanoparticles, which emphasizes their broad-spectrum activity against a variety of bacterial strains [55]. Silver nanoparticles' distinct mechanisms of action, such as damage to membranes and interference with cellular processes, contribute to their effectiveness against a wide range of microbial species [53]. This study provides evidence that silver nanoparticles can be useful in the fight against antibiotic-resistant strains. Similarly, there are several studies that highlight the potential of biogenic nanoparticles (NPs), particularly zinc oxide (ZnO) nanoparticles, as effective antimicrobial agents against multi-drug-resistant bacterial strains [56–58]. While the majority of studies concentrate on antibacterial effectiveness against ATCC strains, we included genome-characterized MDR and clinical strains in our analysis because these are challenging to treat organisms.

Additionally, it has been suggested that *Ocimum sanctum* improves the host's ability to fight off infections by raising interferon, interleukin-4, and T helper cell levels [59]. The antibacterial action of *Ocimum sanctum* leaf extract was suggested by Singhal et al. [60] to be related to its potential to reduce silver ions to silver nanoparticles, which have antibacterial qualities against both Gram-positive and Gram-negative bacteria.

4.3. Cytomorphological study

The morphological scrutiny of HeLa cancer cells was meticulously conducted and documented with a phase contrast microscope, as depicted in the previous study [61]. Pronounced morphological alterations were discerned in both control and HeLa cancer cells subjected to treatment with OsOsAgNPs. During a 24-h exposure period, HeLa cells were treated with varying concentrations of OsAgNPs, specifically 15, 30, 60, 90, and 120 μg/mL (Fig. 4). These results revealed notable morphological transformations characteristic of apoptotic cells, including conspicuous features such as the loss of membrane integrity, cellular shrinkage, and a discernible reduction in cell density [61].

4.4. Cytotoxicity analysis

The MTT assays demonstrating the biosynthesized silver nanoparticles (OsAgNPs) *in-vitro* cytotoxic activity against HeLa cell lines offer fascinating clues about the potential uses of these particles in cancer therapy. According to recent research highlighting the anticancer properties of silver nanoparticles, AgNPs exhibit concentration-dependent cytotoxicity, which causes HeLa cell viability to decrease with increasing concentration and duration of exposure [62,63]. Whereas, in a study conducted by Nandini et al., the researchers investigated the effects of Ag/Fe and Cu/Fe nanoparticles on HeLa cervical cancer cells. Based on their study findings, the researchers concluded that the Cu/Fe nanoparticles exhibited superior anticancer properties compared to the Ag/Fe nanoparticles in the HeLa cervical cancer cell line [64].

Research examining the cytotoxic effects of OsAgNPs on different cancer cell lines has shown a dose-dependent effect on HeLa cell viability, which is supported by the reported decrease in MTT absorbance as AgNPs concentrations rise [65]. The determination of the half-maximal inhibitory concentration (IC50) at 90 g/mL highlights biosynthesized OsAgNPs' potency against HeLa cells in (Fig. 5). This IC50 value falls within a range consistent with other studies' effective anticancer responses [66]. These findings demonstrate the potential of OsAgNPs in cancer therapy, particularly for cervical cancer. The findings of concentration-dependent cytotoxicity in this study call for further investigation into the underlying mechanisms of OsAgNPs-induced cell death, which may involve apoptosis, oxidative stress, or other pathways [67]. There are other studies on the use of nanoparticles on other cancer cells. A study by Shabani et al. describes the development of an innovative nano platform that leverages plasmonic photothermal therapy to selectively target and destroy MCF-7 human breast cancer cells, while also maintaining acceptable biocompatibility and eco-friendly properties [68]. Another study by Abbasi et al. reported that the chitosan-coated green-synthesized Fe3O4@MoS2 core-shell nanoparticles exhibited promising anti-cancer properties against the MCF-7 breast cancer cell line [69]. Furthermore, future research could look into the selectivity of OsAgNPs towards other cancer cells while sparing normal cells, which is important for developing targeted and safe cancer treatment [67].

It has been amply demonstrated that tulsi leaves possess anticancer properties [70]. Eugenol (4200–4970 ppm) is present in high amounts in tulsi leaves. Eugenol, which has an allyl chain, is an alternative to guaiacol. Eugenol is derived from the precursor molecule phenylalanine and is a member of the phenylpropanoids chemical group [71]. Eugenol exhibits anticancer effects through multiple mechanisms, such as inducing cell death, cell cycle arrest, and preventing migration, metastasis, and angiogenesis in various cancer types [72]. In an *in vitro* experiment, just a small amount of eugenol in combination with gemcitabine boosted the medication's effectiveness while having no detrimental effects on healthy cells [73].

4.5. Dual AO/EtBr staining to detect apoptosis

Dual acridine orange/ethidium bromide (AO/EtBr) staining, which has been shown to indicate the apoptotic potential of biogenic silver nanoparticles (OsAgNPs), offers important insights into the mechanistic aspects of OsAgNPs-induced cell death. The treated groups exhibit different cellular responses, while the control group's unique green fluorescence indicates normal, viable cells (Fig. 6). Following OsAgNPs treatment, early-stage apoptotic cells exhibit crescent-shaped or granular yellow-green acridine orange nuclear staining, which is consistent with known apoptotic hallmarks [74]. Chromatin condensation, a hallmark of early-stage apoptosis, is indicated by this staining pattern. Simultaneously, late-stage apoptotic cells that show orange nuclear ethidium bromide staining in a focused and lopsidedly localized manner support apoptotic induction. Increased membrane permeability is linked to this staining pattern and is a common feature of apoptotic cells [75]. Additionally, necrotic cell death is indicated by the observed increase in volume and uneven, orange-red fluorescence at the periphery of cells, highlighting the variety of cellular responses triggered by AgNPs [76]. The complexity of OsAgNPs' interactions with cellular mechanisms is highlighted by their capacity to trigger both necrotic and apoptotic cell death pathways. These results are consistent with recent research showing that silver nanoparticles can induce programmed cell death pathways in cancer cells through apoptosis [66]. This study's dual staining method provides a thorough understanding of the cytotoxic effects of OsAgNPs and supports the evidence for their role in necrosis and apoptosis.

5. Conclusion

OsAgNPs were successfully synthesized using aqueous leaf extract of *Ocimum sanctum* and were characterized by various techniques. Our research findings advance the field of nanomedicine by demonstrating the potent antimicrobial efficacy of silver nanoparticles (OsAgNPs) against genetically confirmed MDR bacterial strains, emphasizing their potential as effective agents in combating bacterial infections. Expanding our focus to oncology, we show that OsAgNPs have a cytotoxic effect on HeLa cells, resulting in morphological changes indicative of apoptosis and a concentration-dependent reduction in cell viability. These results position the OsAgNPs as prospective therapeutic agents with the potential to address the growing challenges posed by antibiotic resistance and cervical cancer. Our goal is to reduce the gap between cutting-edge discoveries achieved in the laboratory and ground-breaking clinical applications by bringing attention to the diverse applications of OsAgNPs and accelerating the ongoing evolution of nanomedicine.

Limitations of the study

Since we carried out our investigation in the Department of Clinical Microbiology, we were not equipped to look into biocomponents and how they interact with OsAgNPs. Additionally, this study was limited to HeLa cell lines. Future research is necessary to build a more effective and focused cancer treatment by examining the selectivity of nanoparticles and broadening the research

emphasis beyond a single cancer cell line.

Funding

This work was supported by the project grant (G01/AGU-5/20) from the Arabian Gulf University, Manama, Kingdom of Bahrain.

Data availability statement

All the original data presented in the study is included in this article.

CRediT authorship contribution statement

Nayeem Ahmad: Writing – review & editing, Writing – original draft, Software, Resources, Methodology, Formal analysis, Data curation, Conceptualization. **Mohammad Azam Ansari:** Methodology, Formal analysis. **Ali Al-Mahmeed:** Methodology, Data curation. **Ronni Mol Joji:** review and editing manuscript, Validation. **Nermin Kamal Saeed:** Resources. **Mohammad Shahid:** Validation, Supervision, Project administration, Funding acquisition, Conceptualization.

Declaration of competing interest

The authors declare that they have no known competing financial interests or personal relationships that could have appeared to influence the work reported in this paper.

Acknowledgement

The authors would like to acknowledge and thank Imam Abdulrahman Bin Faisal University, Dammam, Saudi Arabia, for helping in the characterization of green nanomaterials by using the FTIR, TEM, SEM, and EDX facilities. Nayeem Ahmad gratefully thanks Arabian Gulf University (AGU), Bahrain for providing a Postdoctoral Fellowship. Mohammad Shahid acknowledges and thanks AGU for providing a travel grant for presenting this work at the Canadian Cancer Research Conference (CCRC), organized by the Canadian Cancer Research Alliance (CCRA), Halifax Convention Centre, Halifax, Canada (November 12–14, 2023). The authors also wish to thank the Academic Chair of Clinical Microbiology, and Immunology of His Highness Late Amir of Kuwait Sheikh Jaber Al-Ahmad Al-Sabah for providing necessary help in conducting the research.

Appendix A. Supplementary data

Supplementary data to this article can be found online at https://doi.org/10.1016/j.heliyon.2024.e35486.

References

[1] F. Erci, R. Cakir-Koc, I. Isildak, Green synthesis of silver nanoparticles using Thymbra spicata L. var. spicata (zahter) aqueous leaf extract and evaluation of their morphology-dependent antibacterial and cytotoxic activity, Artificial cells, nanomedicine, and biotechnology 46 (2018) 150–158.
[2] K.D. Bhatte, K.M. Deshmukh, Y.P. Patil, D.N. Sawant, S.-I. Fujita, M. Arai, B.M. Bhanage, Synthesis of powdered silver nanoparticles using hydrogen in aqueous medium, Particuology 10 (2012) 140–143.
[3] G. Akintayo, A. Lateef, M. Azeez, T. Asafa, I. Oladipo, J. Badmus, S. Ojo, J. Elegbede, E. Gueguim-Kana, L. Beukes, Synthesis, bioactivities and cytogenotoxicity of animal Fur-mediated silver nanoparticles, in: IOP Conference Series: Materials Science and Engineering, IOP Publishing, 2020 012041.
[4] A. Allafchian, S. Mirahmadi-Zare, S. Jalali, S. Hashemi, M. Vahabi, Green synthesis of silver nanoparticles using phlomis leaf extract and investigation of their antibacterial activity, Journal of Nanostructure in Chemistry 6 (2016) 129–135.
[5] A. Lateef, M.A. Azeez, T.B. Asafa, T.A. Yekeen, A. Akinboro, I.C. Oladipo, L. Azeez, S.E. Ajibade, S.A. Ojo, E.B. Gueguim-Kana, Biogenic synthesis of silver nanoparticles using a pod extract of Cola nitida: antibacterial and antioxidant activities and application as a paint additive, J. Taibah Univ. Sci. 10 (2016) 551–562.
[6] E. Abdel-Halim, M. El-Rafie, S.S. Al-Deyab, Polyacrylamide/guar gum graft copolymer for preparation of silver nanoparticles, Carbohydrate Polymers 85 (2011) 692–697.
[7] L. Chen, X. Zhou, Y. Shi, B. Gao, J. Wu, T.B. Kirk, J. Xu, W. Xue, Green synthesis of lignin nanoparticle in aqueous hydrotropic solution toward broadening the window for its processing and application, Chem. Eng. J. 346 (2018) 217–225.
[8] S. Iravani, R.S. Varma, Biofactories: engineered nanoparticles via genetically engineered organisms, Green Chem. 21 (2019) 4583–4603.
[9] A.I. Osman, et al., Synthesis of green nanoparticles for energy, biomedical, environmental, agricultural, and food applications: a review, Environ. Chem. Lett. 22 (2024) 841–887, https://doi.org/10.1007/s10311-023-01682-3.
[10] R. Rajan, K. Chandran, S.L. Harper, S.-I. Yun, P.T. Kalaichelvan, Plant extract synthesized silver nanoparticles: an ongoing source of novel biocompatible materials, Ind. Crop. Prod. 70 (2015) 356–373.
[11] N. Freire, R. Barbosa, F. García-Villén, C. Viseras-Iborra, L. Perioli, R. Fialho, E. Albuquerque, Green Chemistry Application in Nanoparticles for Biomedical Therapy, Anticancer Medicine, 2023.
[12] X. Zhang, H. Sun, S. Tan, J. Gao, Y. Fu, Z. Liu, Hydrothermal synthesis of Ag nanoparticles on the nanocellulose and their antibacterial study, Inorg. Chem. Commun. 100 (2019) 44–50.
[13] Z.-u.-R. Mashwani, T. Khan, M.A. Khan, A. Nadhman, Synthesis in plants and plant extracts of silver nanoparticles with potent antimicrobial properties: current status and future prospects, Appl. Microbiol. Biotechnol. 99 (2015) 9923–9934.

[14] S. Fahimirad, F. Ajalloueian, M. Ghorbanpour, Synthesis and therapeutic potential of silver nanomaterials derived from plant extracts, Ecotoxicology and environmental safety 168 (2019) 260–278.
[15] P.V. Kumar, S. Pammi, P. Kollu, K. Satyanarayana, U. Shameem, Green synthesis and characterization of silver nanoparticles using Boerhaavia diffusa plant extract and their anti bacterial activity, Ind. Crop. Prod. 52 (2014) 562–566.
[16] H. Jan, M. Shah, H. Usman, M.A. Khan, M. Zia, C. Hano, B.H. Abbasi, Biogenic synthesis and characterization of antimicrobial and antiparasitic zinc oxide (ZnO) nanoparticles using aqueous extracts of the Himalayan Columbine (Aquilegia pubiflora), Frontiers in Materials 7 (2020) 249.
[17] K. Jyoti, M. Baunthiyal, A. Singh, Characterization of silver nanoparticles synthesized using Urtica dioica Linn. leaves and their synergistic effects with antibiotics, Journal of Radiation Research and Applied Sciences 9 (2016) 217–227.
[18] S.N. Kharat, V.D. Mendhulkar, Synthesis, characterization and studies on antioxidant activity of silver nanoparticles using Elephantopus scaber leaf extract, Mater. Sci. Eng. C 62 (2016) 719–724.
[19] A.-R. Phull, Q. Abbas, A. Ali, H. Raza, M. Zia, I.-u. Haq, Antioxidant, cytotoxic and antimicrobial activities of green synthesized silver nanoparticles from crude extract of Bergenia ciliata, Future Journal of Pharmaceutical Sciences 2 (2016) 31–36.
[20] M. Shah, S. Nawaz, H. Jan, N. Uddin, A. Ali, S. Anjum, N. Giglioli-Guivarc'h, C. Hano, B.H. Abbasi, Synthesis of bio-mediated silver nanoparticles from Silybum marianum and their biological and clinical activities, Mater. Sci. Eng. C 112 (2020) 110889.
[21] S. Ahmed, M. Ahmad, B.L. Swami, S. Ikram, Green synthesis of silver nanoparticles using Azadirachta indica aqueous leaf extract, Journal of radiation research and applied sciences 9 (2016) 1–7.
[22] J. O'Neill, Tackling Drug-Resistant Infections Globally: Final Report and Recommendations, 2016.
[23] P. Raghav, M. Saini, Antimicrobial Propeties of Tulsi (Ocimum Sanctum), vol. 7, 2018, pp. 20–32, https://doi.org/10.24214/IJGHC/HC/7/1/02032.
[24] S. Shiwakoti, O. Saleh, S. Poudyal, A. Barka, Y. Qian, V.D. Zheljazkov, Yield, composition and antioxidant capacity of the essential oil of sweet basil and holy basil as influenced by distillation methods, Chem. Biodivers. (2017) e1600417, https://doi.org/10.1002/CBDV.201600417.
[25] T.P.C. Ezeorba, et al., Health and therapeutic potentials of Ocimum essential oils: a review on isolation, phytochemistry, biological activities, and future directions, J. Essent. Oil Res. 36 (3) (2024) 271–290, https://doi.org/10.1080/10412905.2024.2338117.
[26] N. Ahmad, R.M. Joji, M. Shahid, Evolution and implementation of One Health to control the dissemination of antibiotic-resistant bacteria and resistance genes: a review, Front. Cell. Infect. Microbiol. 12 (2023) 1065796.
[27] J. Ramamurthy, B.A. Deepika, Anti-microbial activity of *Ocimum sanctum L.* gel against black pigmented microbes, Bioinformation 20 (2024) 277–281, https://doi.org/10.6026/973206300200277.
[28] T. Khaliq, M.A. Waseem, A.M. Lone, Q.P. Hassan, Oscimum sanctum extract inhibits growth of Gram positive and Gram negative bacterial strains, Microb. Pathog. 118 (2018) 211–213, https://doi.org/10.1016/j.micpath.2018.03.040.
[29] A. Kanchana, M. Balakrishna, Anti-cancer effect of saponins isolated from Solanum trilobatum leaf extract and induction of apoptosis in human larynx cancer cell lines, Int. J. Pharm. Pharmaceut. Sci. 3 (2011) 356–364.
[30] A. Jemal, A. Thomas, T. Murray, M. Thun, Cancer statistics, Ca-Cancer J. Clin. 52 (2002) 23–47, 2002.
[31] R. Kumari, A.K. Saini, A. Kumar, R.V. Saini, Apoptosis induction in lung and prostate cancer cells through silver nanoparticles synthesized from Pinus roxburghii bioactive fraction, JBIC Journal of Biological Inorganic Chemistry 25 (2020) 23–37.
[32] S.P. Singh, A. Mishra, R.K. Shyanti, R.P. Singh, A. Acharya, Silver nanoparticles synthesized using Carica papaya leaf extract (AgNPs-PLE) causes cell cycle arrest and apoptosis in human prostate (DU145) cancer cells, Biol. Trace Elem. Res. 199 (2021) 1316–1331.
[33] S.F. Hashemi, N. Tasharrofi, M.M. Saber, Green synthesis of silver nanoparticles using Teucrium polium leaf extract and assessment of their antitumor effects against MNK45 human gastric cancer cell line, J. Mol. Struct. 1208 (2020) 127889.
[34] K. Aruna, V.M. Sivaramakrishnan, Anticarcinogenic effects of some Indian plant Products, Food Chem. Toxicol. 30 (1992) 953–956, https://doi.org/10.1016/0278-6915(92)90180-S.
[35] A.M. Luke, et al., An in vitro study of Ocimum sanctum as a chemotherapeutic agent on oral cancer cell-line, Saudi J. Biol. Sci. 28 (1) (2021) 887–890, https://doi.org/10.1016/j.sjbs.2020.11.030.
[36] S. Kumari, et al., Ocimum sanctum: the journey from sacred herb to functional food, Recent advances in food, nutrition & agriculture 15 (2024), https://doi.org/10.2174/012772574X290140240130101117.
[37] M.M. Cohen, Tulsi - Ocimum sanctum: a herb for all reasons, J. Ayurveda Integr. Med. 5 (4) (2014) 251–259, https://doi.org/10.4103/0975-9476.146554.
[38] M. Shahid, et al., Molecular screening of carbapenem-resistant K. pneumoniae (CRKP) clinical isolates for concomitant occurrence of beta-lactam genes (CTX-M, TEM, and SHV) in the kingdom of Bahrain, J. Clin. Med. 12 (24) (2023) 7522, https://doi.org/10.3390/jcm12247522, 5.
[39] M. Shahid, et al., Clinical carbapenem-resistant Klebsiella pneumoniae isolates simultaneously harboring blaNDM-1, blaOXA types and qnrS genes from the Kingdom of Bahrain: resistance profile and genetic environment, Front. Cell. Infect. Microbiol. 12 (2022) 1033305, https://doi.org/10.3389/fcimb.2022.1033305.
[40] M.A. Ansari, R. Govindasamy, M.Y. Begum, M. Ghazwani, A. Alqahtani, M.N. Alomary, Y.F. Jamous, S.A. Alyahya, S. Asiri, F.A. Khan, Bioinspired ferromagnetic CoFe2O4 nanoparticles: potential pharmaceutical and medical applications, Nanotechnol. Rev. 12 (2023) 20230575.
[41] B. Sadeghi, A. Rostami, S. Momeni, Facile green synthesis of silver nanoparticles using seed aqueous extract of Pistacia atlantica and its antibacterial activity, Spectrochim. Acta Mol. Biomol. Spectrosc. 134 (2015) 326–332.
[42] S. Priya, M.S. Peddha, Physicochemical characterization, polyphenols and flavonoids of different extracts from leaves of four varieties of tulsi (Ocimum sp.), South Afr. J. Bot. 159 (2023) 381–395.
[43] H. Skaltsa, O. Tzakou, M. Singh, Note polyphenols of Ocimum sanctum from Suriname, Pharmaceut. Biol. 37 (1999) 92–94.
[44] R.R. Jagtap, A. Garud, S.S. Puranik, M. Rudrapal, M.A. Ansari, M.N. Alomary, M. Alshamrani, A. Salawi, Y. Almoshari, J. Khan, Biofabrication of silver nanoparticles (AgNPs) using embelin for effective therapeutic management of lung cancer, Front. Nutr. 9 (2022) 960674.
[45] A.-W. Ajlouni, E.H. Hamdan, R.A.E. Alshalawi, M.R. Shaik, M. Khan, M. Kuniyil, A. Alwarthan, M.A. Ansari, M. Khan, H.Z. Alkhathlan, Green synthesis of silver nanoparticles using aerial part extract of the Anthemis pseudocotula boiss. plant and their biological activity, Molecules 28 (2022) 246.
[46] K. Sharma, et al., Green synthesis of silver nanoparticles using Ocimum gratissimum leaf extract: characterization, antimicrobial activity and toxicity analysis, J. Plant Biochem. Biotechnol. 29 (2020) 213–224.
[47] S.C. Daniel, et al., Green synthesis (Ocimum tenuiflorum) of silver nanoparticles and toxicity studies in zebra fish (Danio rerio) model, Int. J. Nanosci. Nanotechnol. 2 (2011) 103–117.
[48] A. Alsalhi, et al., Biogenic fabrication and multifunctional therapeutic applications of silver nanoparticles synthesized from rose petal extract, Nanotechnol. Rev. 13 (1) (2024) 20240043, 27.
[49] J.T. Smith, E.M. Eckhardt, N.B. Hansel, T. Rahmani Eliato, I.W. Martin, C.P. Andam, Genome evolution of invasive methicillin-resistant Staphylococcus aureus in the Americas, Microbiol. Spectr. 10 (2022) e00201, 00222.
[50] C.H. Barros, S. Fulaz, D. Stanisic, L. Tasic, Biogenic nanosilver against multidrug-resistant bacteria (MDRB), Antibiotics 7 (2018) 69.
[51] T.C. Dakal, A. Kumar, Mechanistic basis of antimicrobial actions of silver nanoparticles, Front. Microbiol. 7 (2016) 231711.
[52] R. Singh, P. Wagh, S. Wadhwani, S. Gaidhani, A. Kumbhar, J. Bellare, B.A. Chopade, Synthesis, optimization, and characterization of silver nanoparticles from Acinetobacter calcoaceticus and their enhanced antibacterial activity when combined with antibiotics, Int. J. Nanomed. (2013) 4277–4290.
[53] R.Y. Pelgrift, A.J. Friedman, Nanotechnology as a therapeutic tool to combat microbial resistance, Adv. Drug Deliv. Rev. 65 (2013) 1803–1815.
[54] M. Rai, A. Yadav, A. Gade, Silver nanoparticles as a new generation of antimicrobials, Biotechnol. Adv. 27 (2009) 76–83.
[55] T. Bruna, F. Maldonado-Bravo, P. Jara, N. Caro, Silver nanoparticles and their antibacterial applications, Int. J. Mol. Sci. 22 (2021) 7202.
[56] Y. Chan, et al., Green synthesis of ZnO nanoparticles using the mangosteen (Garcinia mangostana L.) leaf extract: comparative preliminary in vitro antibacterial study, Green Process. Synth. 13 (1) (2024) 20230251, https://doi.org/10.1515/gps-2023-0251.
[57] V. Selvanathan, et al., Synthesis, characterization, and preliminary in vitro antibacterial evaluation of ZnO nanoparticles derived from soursop (Annona muricata L.) leaf extract as a green reducing agent, J. Mater. Res. Technol. 20 (2022) 2931–2941, https://doi.org/10.1016/j.jmrt.2022.08.028.

[58] E. Thaninayagam, Antibacterial study of silver nanoparticles synthesized using Strychnos potatorum(linn)– Green synthesis method, in: Materials Today: Proceedings, vol. 68, 2022, pp. 448–453, https://doi.org/10.1016/j.matpr.2022.07.118.
[59] S. Mondal, et al., Double-blinded randomized controlled trial for immunomodulatory effects of Tulsi (Ocimum sanctum Linn.) leaf extract on healthy volunteers, J. Ethnopharmacol. 3 (2011) 452–456.
[60] G. Singhal, et al., Biosynthesis of silver nanoparticles using Ocimum sanctum (Tulsi) leaf extract and screening its antimicrobial activity, J Nanopart Res 13 (2011) 2981–2988.
[61] A. Belashov, A. Zhikhoreva, T. Belyaeva, N. Nikolsky, I. Semenova, E. Kornilova, O. Vasyutinskii, Quantitative assessment of changes in cellular morphology at photodynamic treatment in vitro by means of digital holographic microscopy, Biomed. Opt Express 10 (2019) 4975–4986.
[62] P. Singh, S. Pandit, J. Garnæs, S. Tunjic, V.R. Mokkapati, A. Sultan, A. Thygesen, A. Mackevica, R.V. Mateiu, A.E. Daugaard, Green synthesis of gold and silver nanoparticles from Cannabis sativa (industrial hemp) and their capacity for biofilm inhibition, Int. J. Nanomed. (2018) 3571–3591.
[63] A. Corciovă, C. Mircea, A.F. Burlec, A. Fifere, I.T. Moleavin, A. Sarghi, C. Tuchiluș, B. Ivănescu, I. Macovei, Green synthesis and characterization of silver nanoparticles using a Lythrum salicaria extract and in vitro exploration of their biological activities, Life 12 (2022) 1643.
[64] R. Raja Nandhini, et al., Green synthesis of silver/iron(Ag/Fe) and copper/iron(Cu/Fe) nanoparticles for cytotoxic investigation on henrietta lacks(HeLa) cancer cell, in: S. Mavinkere Rangappa, S. Siengchin (Eds.), Proceedings of the International Symposium on Lightweight and Sustainable Polymeric Materials (LSPM23). LSPM 2023, Springer Proceedings in Materials, 2023, p. 32, https://doi.org/10.1007/978-981-99-5567-1_7.
[65] I. Khan, K. Saeed, I. Khan, Nanoparticles: properties, applications and toxicities, Arab. J. Chem. 12 (2019) 908–931.
[66] S. Gurunathan, J.W. Han, V. Eppakayala, M. Jeyaraj, J.-H. Kim, Cytotoxicity of biologically synthesized silver nanoparticles in MDA-MB-231 human breast cancer cells, BioMed Res. Int. (2013) 2013.
[67] X.-F. Zhang, Z.-G. Liu, W. Shen, S. Gurunathan, Silver nanoparticles: synthesis, characterization, properties, applications, and therapeutic approaches, Int. J. Mol. Sci. 17 (2016) 1534.
[68] L. Shabani, et al., An investigation into green synthesis of Ru template gold nanoparticles and the in vitro photothermal effect on the MCF-7 human breast cancer cell line, Appl. Phys. A 129 (2023) 564, https://doi.org/10.1007/s00339-023-06832-6.
[69] M. Abbasi, et al., Allium hooshidaryae (Alliaceae)-based green-synthesized Fe3O4@MoS2 core–shell nanoparticles coated with chitosan and investigating their biological properties, Appl. Phys. A 130 (2024) 284, https://doi.org/10.1007/s00339-024-07440-8.
[70] B. Salehi, et al., Thymol, thyme, and other plant sources: health and potential uses, Phytother Res. 32 (2018) 1688–1706, https://doi.org/10.1002/ptr.6109.
[71] M.R. Hasan, et al., An update on the therapeutic anticancer potential of Ocimum sanctum L. "Elixir of life", Molecules.25 28 (3) (2023) 1193, https://doi.org/10.3390/molecules28031193. PMID: 36770859; PMCID: PMC9919305.
[72] A.T. Zari, T.A. Zari, K.R. Hakeem, Anticancer properties of eugenol: a review, Molecules 26 (2021) 7407, https://doi.org/10.3390/molecules26237407.
[73] U. Vora, et al., Effects of eugenol on the behavioral and pathological progression in the MPTP-induced Parkinson's disease mouse model, Drug Discov. Ther. 16 (2022) 154–163, https://doi.org/10.5582/ddt.2022.0102.
[74] G. Kroemer, L. Galluzzi, P. Vandenabeele, J. Abrams, E.S. Alnemri, E. Baehrecke, M. Blagosklonny, W. El-Deiry, P. Golstein, D. Green, Classification of cell death: recommendations of the nomenclature committee on cell death 2009, Cell Death Differ. 16 (2009) 3–11.
[75] B. Fadeel, Programmed cell clearance, Cellular and Molecular Life Sciences CMLS 60 (2003) 2575–2585.
[76] M. Sajjadi, M. Nasrollahzadeh, B. Jaleh, G.J. Soufi, S. Iravani, Carbon-based nanomaterials for targeted cancer nanotherapy: recent trends and future prospects, J. Drug Target. 29 (2021) 716–741.